

# THE EFFECTS OF DIFFERENT TYPES OF WAVELETS ON IMAGE FUSION

Gang Hong, Yun Zhang  
Department of Geodesy and Geomatics Engineering  
University of New Brunswick, Fredericton, New Brunswick, Canada E3B 5A3  
v5z78@unb.ca  
YunZhang@UNB.ca

**KEY WORDS:** fusion, integration, multiresolution, multisensor, multispectral, resolution

## ABSTRACT:

Image fusion is a tool for integrating a high-resolution panchromatic image with a multispectral image, in which the resulting fused image contains both the high-resolution spatial information of the panchromatic image and the color information of the multispectral image. Wavelet transformation, originally a mathematical tool for signal processing, is now popular in the field of image fusion. Recently, many image fusion methods based on wavelet transformation have been published. The wavelets used in image fusion can be categorized into three general classes: Orthogonal, Biorthogonal and Nonorthogonal. Although these wavelets share some common properties, each wavelet leads to unique image decomposition and a reconstruction method which leads to differences among wavelet fusion methods.

This paper focuses on the comparison of the image fusion methods which utilize the wavelets of the above three general classes. The typical wavelets from the above three general classes – Daubechies (Orthogonal), spline biorthogonal (Biorthogonal), and  $\hat{A}$  trous (Nonorthogonal) – are selected as the mathematical models to implement image fusion algorithms.

When wavelet transformation alone is used for image fusion, the fusion result is often not good. However, if wavelet transform and IHS transform are integrated, better fusion results may be achieved. Because the substitution in IHS transform is limited to only the intensity component, integrating of the wavelet transform to improve or modify the intensity and the IHS transform to fuse the image can make the fusion process simpler and faster. This integration can also better preserve color information. The fusion method based on the above IHS and wavelet integration concept is employed in this paper. IKONOS image data are used to evaluate the three different kinds of wavelet fusion methods mentioned above. The fusion results are compared graphically, visually, and statistically.

## 1. INTRODUCTION

Image fusion is a tool for integrating a high-resolution panchromatic image with a multispectral image, in which the resulting fused image contains both the high-resolution spatial information of the panchromatic image and the color information of the multispectral image. More and more high-resolution sensors appear as the technology develops, and correspondingly, a variety of high-resolution images are available; however, because of the benefits of image fusion, it is still a popular method to interpret image data. Pohl and Genderen (1998) have concluded that image fusion has the following functions by studying the literature: sharpen images; improve geometric corrections, provide stereo-viewing capabilities for stereophotogrammetry; enhance certain features not visible in either of the single data alone; complement data sets for improved classification; detect changes using multitemporal data; substitute missing information (e.g., clouds-VIR, shadows-SAR) in one image with signals from another sensor image; replace defective data.

Wavelet is a relative new fusion method, which is a mathematical tool initially designed for signal processing. Because it provides multiresolution and multiscale analysis function, image fusion can be implemented in the wavelet transform domain. This feature cannot be replaced by any traditional fusion methods. Many papers about image fusion based on wavelet transform have been published in recent years (Yocky, 1995; Li, et al, 1995; Yocky, 1996; Zhou et al, 1998; Núñez, et al., 1999; Ranchin et al, 2000; Aiazzi, et.al, 2002). Until now, the wavelets that have been used in image fusion domain can generally be categorized into three typical different types: Daubechies (Orthogonal), spline biorthogonal (Biorthogonal) and  $\hat{A}$  trous (Nonorthogonal). This paper focuses on these three different wavelets and compares their fusion results.

The rest of this paper is organized as follows: general description of wavelet theory used in the image fusion is given in section 2; section 3 is the experimental results and comparison; the conclusion is provided in section 4.

## 2. WAVELET USED IN THE IMAGE FUSION

## 2.1 Basic introduction to related theory

In wavelet transformation, the basis functions are a set of dilated and translated scaling functions:

$$\varphi_{j,k}(n) = 2^{j/2} \varphi(2^j n - k) \quad (1)$$

and a set of dilated and translated wavelet functions:

$$\psi_{j,k}(n) = 2^{j/2} \psi(2^j n - k) \quad (2)$$

where  $\varphi(n)$  and  $\psi(n)$  are the scaling function and the mother wavelet function respectively. One property that the basis function must satisfy is that both the scaling function and the wavelet function at level  $j$  can be expressed as a linear combination of the scaling functions at the next level  $j+1$ :

$$\varphi_{j,k}(n) = \sum_m h(m - 2k) \varphi_{j+1,m}(n) \quad (3)$$

and

$$\psi_{j,k}(n) = \sum_m g(m - 2k) \varphi_{j+1,m}(n) \quad (4)$$

where  $h(m)$  and  $g(m)$  are called the scaling filter and the wavelet filter respectively.

For any continuous function, it can be represented by the following expansion, defined in a given scaling function and its wavelet derivatives (Burrus, et.al.1998):

$$f(n) = \sum_k c_{j_0}(k) \varphi_{j_0,k}(n) + \sum_{j=j_0}^{\infty} \sum_k d_j(k) \psi_{j,k}(n) \quad (5)$$

The fast Discrete Wavelet Transform (DWT) can be expressed as follows:

$$c_{j+1}(k) = \sum_n c_j(n) h^*(n - 2k) \quad (6)$$

$$d_{j+1}(k) = \sum_n c_j(n) g^*(n - 2k) \quad (7)$$

The scaling filter  $h^*(n)$  is a low pass filter extracting the approximate coefficients,  $c_{j+1}(k)$ , with  $c_0(n) = f(n)$ , while the wavelet filter  $g^*(n)$  is a high-pass filter extracting the detail coefficients  $d_{j+1}(k)$ . The coefficients are downsampled (i.e. only every other coefficient is taken).

The reconstruction formulas are given by:

$$c_j(k) = \sum_n (c_{j+1}(n) h^*(n - 2k) + d_{j+1}(n) g^*(n - 2k)) \quad (8)$$

Generally, discrete wavelet is introduced by multi-resolution analysis. Let  $L^2(\mathbb{R})$  be the Hilbert space of functions, a multiresolution analysis (MRA) of  $L^2(\mathbb{R})$  is a sequence of closed subspaces  $V_j$ ,  $j \in \mathbb{Z}$  ( $\mathbb{Z}$  is the set of integers), of  $L^2(\mathbb{R})$  satisfying the following six properties (Mallat, 1989):

1. The subspaces are nested:  $V_j \subset V_{j+1} \quad \forall j \in \mathbb{Z}$
2. Separation:  $\bigcap_{j \in \mathbb{Z}} V_j = \{0\}$
3. The union of the subspaces generate  $L^2(\mathbb{R})$ :  $\overline{\bigcup_{j \in \mathbb{Z}} V_j} = L^2(\mathbb{R})$
4. Scale invariance:  $f(t) \in V_j \Leftrightarrow f(2t) \in V_{j+1} \quad \forall j \in \mathbb{Z}$
5. Shift invariance:  $f(t) \in V_0 \Leftrightarrow f(t - k) \in V_0 \quad \forall k \in \mathbb{Z}$
6.  $\exists \phi \in V_0$ , the scaling function, so that  $\{\phi(2^{-j/2} - k) | k \in \mathbb{Z}\}$  is a Riesz basis of  $V_0$ .

There is also a related sequence of wavelet subspaces  $W_j$  of  $L^2(\mathbb{R})$ ,  $\forall j \in \mathbb{Z}$ , where  $W_j$  is the orthogonal complement of  $V_j$  in  $V_{j+1}$ . Then,  $V_{j-1} = V_j \oplus W_j$ , where  $\oplus$  is the direct sum.

The above applies to about one-dimension situation; for two-dimension situation, the scaling function is defined as:

$$\Phi(x, y) = \phi(x)\phi(y) \quad (9)$$

Vertical wavelet:

$$\Psi^1(x, y) = \phi(x)\psi(y) \quad (10)$$

Horizontal wavelet:

$$\Psi^2(x, y) = \psi(x)\phi(y) \quad (11)$$

Diagonal wavelet

$$\Psi^3(x, y) = \psi(x)\psi(y) \quad (12)$$

$\Phi(x, y)$  can be thought of as a 2-D scaling function,  $\Psi^1(x, y)$ ,  $\Psi^2(x, y)$ ,  $\Psi^3(x, y)$  are the three 2-D wavelet functions.

For the two-dimension image, the transform can be expressed by the follows:

$$a_{j-1}(x, y) = \sum_{c=-\infty}^{\infty} \sum_{r=-\infty}^{\infty} h(c - 2x)h(r - 2y)f_j(c, r) \quad (13)$$

$$d_{j-1}^1(x, y) = \sum_{c=-\infty}^{\infty} \sum_{r=-\infty}^{\infty} g(c - 2x)h(r - 2y)f_j(c, r) \quad (14)$$

$$d_{j-1}^2(x, y) = \sum_{c=-\infty}^{\infty} \sum_{r=-\infty}^{\infty} h(c - 2x)g(r - 2y)f_j(c, r) \quad (15)$$

$$d_{j-1}^3(x, y) = \sum_{c=-\infty}^{\infty} \sum_{r=-\infty}^{\infty} g(c - 2x)g(r - 2y)f_j(c, r) \quad (16)$$

Here,  $a_{j-1}$  corresponds to the  $j-1$  level approximate image, and  $d_{j-1}^1, d_{j-1}^2, d_{j-1}^3$  are the horizontal, vertical, and diagonal subimages, respectively.

## 2.2 Different wavelet used in the image fusion

### 2.2.1 Orthogonal wavelet

The dilations and translations of the scaling function  $\{\phi_{j,k}(x)\}$  constitute a basis for  $V_j$  and, similarly,  $\{\psi_{j,k}(x)\}$  for  $W_j$ , if the  $\phi_{j,k}(x)$  and  $\psi_{j,k}(x)$  are orthonormal, it includes the following properties:

$$V_j \perp W_j \quad (17)$$

$$\langle \phi_{j,l}, \phi_{j,l'} \rangle = \delta_{l,l'}, \langle \psi_{j,l}, \psi_{j,l'} \rangle = \delta_{l,l'},$$

$$\langle \phi_{j,l}, \psi_{j,l'} \rangle = 0 \quad (18)$$

The orthogonality property puts a strong limitation on the construction of wavelets. For example, it is hard to find any wavelets that are compactly supported, symmetric, and orthogonal.

### 2.2.2 Biorthogonal wavelet

If the orthogonality condition is relaxed to biorthogonality conditions, wavelets with some special properties that are not possible with orthogonal wavelets can be obtained. In the biorthogonal transform, there are two multi-resolution analyses, a primal and a dual:

$$\text{Primal: } V_j, W_j, \phi_{j,k}, \psi_{j,k},$$

$$\text{Dual: } \tilde{V}_j, \tilde{W}_j, \tilde{\phi}_{j,k}, \tilde{\psi}_{j,k}.$$

The dilations and translations of the scaling function  $\{\tilde{\phi}_{j,k}(x)\}$  constitute a basis for  $\tilde{V}_j$  and, similarly,  $\{\tilde{\psi}_{j,k}(x)\}$  for  $\tilde{W}_j$ ; the biorthogonality conditions imply:

$$\tilde{V}_j \perp W_j, V_j \perp \tilde{W}_j \quad (19)$$

$$\langle \tilde{\phi}_{j,l}, \phi_{j,l'} \rangle = \delta_{l,l'}, \langle \tilde{\psi}_{j,l}, \psi_{j,l'} \rangle = \delta_{j,j'} \delta_{l,l'},$$

$$\langle \tilde{\psi}_{j,l}, \phi_{j,l'} \rangle = 0, \langle \tilde{\phi}_{j,l}, \psi_{j,l'} \rangle = 0 \quad (20)$$

For the biorthogonal transform, perfect reconstruction is available. Orthogonal wavelets give orthogonal matrices and unitary transforms; biorthogonal wavelets give invertible matrices and perfect reconstruction. For the biorthogonal wavelet filter, the low pass and the high pass filters do not have the same length. The low pass filter is always symmetric, while the high pass filter could be either symmetric or anti-symmetric.

### 2.2.3 A trous (Nonorthogonal wavelet)

A trous (with holes) is a kind of Nonorthogonal wavelet which is different from orthogonal and biorthogonal. It is a "stationary" or redundant transform; i.e., decimation is not implemented during the process of wavelet transform, while orthogonal and biorthogonal wavelet transform can be carried

out using either decimation or undecimation mode. Compared with other fusion-based wavelet transform, this method is relatively easy to implement. The limitation is that it will use a lot of computer memory.

## 3. EXPERIMENTAL RESULTS AND COMPARISON

Corresponding to the different wavelets, six kinds of wavelet methods are implemented to test their fusion results. Decimation and undecimation cases are considered in the orthogonal and biorthogonal wavelet, respectively. They are orthogonal wavelet fusion with decimation (called ORTH method), orthogonal wavelet fusion without decimation (simply called UORTH), biorthogonal wavelet fusion with decimation (simply called BIOR), biorthogonal wavelet fusion without decimation (simply called UBIOR), wavelet fusion based on the A trous (simply called ATRO), wavelet fusion based on wavelet and IHS transformation (simply called WIHS)(Hong and Zhang, 2003). The undecimation orthogonal wavelet is used in the WIHS fusion method. The orthogonal and biorthogonal wavelet coefficients are listed in Table 1 and Table 2, respectively. A subset of IKONOS data (512 pixels by 512 pixels) is used to evaluate the fusion algorithm. The fusion results are listed in Figure 3~Figure 8. Figure 1 is the original IKONOS panchromatic image, Figure 2 is the original IKONOS multispectral image, Figure 3 is the fusion result of orthogonal wavelet fusion with decimation, Figure 4 is the fusion result of biorthogonal wavelet with decimation, Figure 5 is the fusion result of orthogonal wavelet without decimation, Figure 6 is the fusion result of biorthogonal wavelet without decimation, Figure 7 is the fusion result of A trous wavelet, Figure 8 is the fusion result of the IHS transformation combined with wavelet.

From the point of visual comparison, ORTH result is similar to BIOR result, UORTH result is similar to UBIOR; while there exists apparent color distortion in ORTH and BIOR, the degree of color distortion in UORTH and UBIOR is lighter than that in ORTH and BIOR; however, the spatial detail information in ORTH and BIOR is more plentiful than that in UORTH and UBIOR. Combining the spatial and color together, the rank of the fusion result is WIHS, ATRO, UORTH (UBIOR), ORTH (BIOR). The biorthogonal and orthogonal difference cannot be differentiated from the fusion result. The decimation and undecimation can be differentiated from the fusion result.

From the point of statistical analysis, Table 3 lists the correlation coefficients between fusion result and original multispectral image, and Table 4 lists the correlation coefficients between fusion result and original panchromatic image. In Table 3, it can be found that WIHS is highest, the second highest is ATRO, the third is UORTH (UBIOR), the lowest is ORTH (BIOR). In Table 4, the highest is ORTH

(BIOR), the second is WIHS, the third is ATRO, and the lowest is UORTH (UBIOR). The statistical

analysis results correspond to the visual comparison result.



Figure 1. Original Panchromatic image



Figure 2. Original Multispectral image



Figure 3. ORTH fusion result



Figure 4. BIOR fusion result



Figure 5. UORTH fusion result



Figure 6. UBIOR fusion result

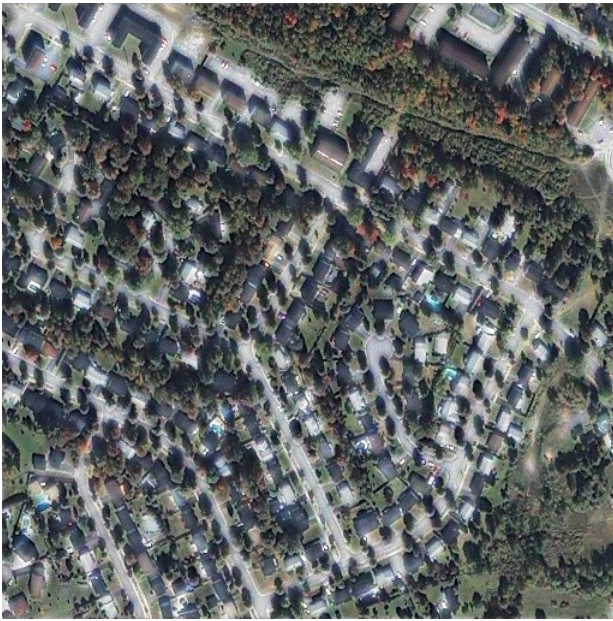


Figure 7. ATROUS fusion result



Figure 8. WIHS fusion result

Table 1. Orthogonal wavelet filter coefficients

LD	-0.0106	0.0329	0.0308	-0.1870	-0.0280	0.6309	0.7148	0.2304
HD	-0.2304	0.7148	-0.6309	-0.0280	0.1870	0.0308	-0.0329	-0.0106
LR	0.2304	0.7148	0.6309	-0.0280	-0.1870	0.0308	0.0329	-0.0106
HR	-0.0106	-0.0329	0.0308	0.1870	-0.0280	-0.6309	0.7148	-0.2304

Here, LD means decomposition low-pass filter, HD means decomposition high-pass filter. LR means reconstruction low-pass filter, and HR means reconstruction high-pass filter, the same to Table 2.

Table 2. Biorthogonal wavelet filter coefficients

LD	0	0.0378	-0.0238	-0.1106	0.3774	0.8527	0.3774	-0.1106	-0.0238	0.0378
HD	0	-0.0645	0.0407	0.4181	-0.7885	0.4181	0.0407	-0.0645	0	0
LR	0	-0.0645	-0.0407	0.4181	0.7885	0.4181	-0.0407	-0.0645	0	0

HR	0	-0.0378	-0.0238	0.1106	0.3774	-0.8527	0.3774	0.1106	-0.0238	0.0378
----	---	---------	---------	--------	--------	---------	--------	--------	---------	--------

Table 3. Correlation coefficients between the original multispectral file and fusion result

	ORTH	BIOR	UORTH	UBIOR	ATRO	WIHS
Multispectral image R	0.743	0.757	0.823	0.813	0.864	0.897
Multispectral image G	0.726	0.750	0.805	0.817	0.859	0.886
Multispectral image B	0.714	0.708	0.813	0.804	0.803	0.804

Table 4. Correlation coefficients between the original panchromatic file and fusion result

	ORTH	BIOR	UORTH	UBIOR	ATRO	WIHS
Panchromatic image	0.876	0.872	0.735	0.725	0.793	0.819
	0.879	0.876	0.728	0.714	0.787	0.846
	0.834	0.832	0.704	0.704	0.732	0.721

#### 4. CONCLUSION

This paper has described six kinds of wavelet-related fusion methods. Their results are compared and ranked through both visual and statistical comparison. When wavelet transformation alone is used for image fusion, the fusion result is often not good. However, if the wavelet transform and the IHS transform are integrated, better fusion results may be achieved. Because the substitution in IHS transform is limited to only the intensity component, integrating of the wavelet transform to improve or modify the intensity and the IHS transform to fuse the image can make the fusion process simpler and faster. This integration can also better preserve color information. Moreover, from the appearance of their results, the WIHS fusion result is continuous, while others' results resemble those produced by a high-pass filter.

#### REFERENCES

Aiazzi, B., L. Alparone, S. Baronti & A. Garzelli, 2002. Context driven fusion of high spatial and spectral resolution images based on oversampled multiresolution analysis. *IEEE Transactions on Geoscience and Remote Sensing*, vol.40, no.10, pp.2300-2312.

Burrus, C.S., Gopinath, R.A., and Guo, H., 1998. *Introduction to Wavelets and Wavelet Transforms*, Prentice-Hall, Inc. New Jersey.

Mallat, G. S., 1989. A theory for multiresolution signal decomposition: The wavelet representation. *IEEE Transactions of Pattern Analysis and Machine Intelligence*, 11(7): 674--693, July 1989.

Hong, G. and Y. Zhang (2003). High resolution image fusion based on Wavelet and IHS transformations. In: *Proceedings of the IEEE/ISPRS joint Workshop on "Remote Sensing and Data Fusion over Urban Areas"*, Berlin, 2003; pp. 99 - 104.

Li, H., B.S. Manjunath, and S.K. Mitra, "Multisensor image fusion using the wavelet transform," *Graph. Models Image Process*, vol. 57, no. 3, pp. 235-245, 1995.

Pohl, C. and Van Genderen, J. L., 1998. *Multisensor image fusion in remote sensing: concepts, methods,*

*and applications*. International Journal of Remote Sensing, Vol. 19, pp 823-854

Ranchin, T. and Wald, L., 2000. Fusion of High Spatial and Spectral Resolution images: The ARSIS Concept and Its Implementation. *Photogrammetric Engineering & Remote sensing* Vol. 66, pp. 49-61.

Yocky, D. A., 1995. Image merging and data fusion using the discrete two-dimensional wavelet transform. *J. Opt. Soc. Am. A.*, Vol. 12, No 9, pp. 1834-1841.

Yocky, D. A., 1996. Multiresolution Wavelet Decomposition Image Merger of Landsat Thematic Mapper and SPOT Panchromatic Data. *Photogrammetric Engineering & Remote sensing* Vol. 62, No. 3, pp295-303.

Zhou, J., Civco, D. L., and Silander, J. A., 1998. A wavelet transform method to merge Landsat TM and SPOT panchromatic data. *International Journal of Remote Sensing*, Vol. 19, No. 4, pp. 743-757.

Núñez, J., X. Otazu, O. Fors, A. Prades, V. Palà, and R. Arbiol, "Multiresolution-based image fusion with additive wavelet decomposition," *IEEE Trans. Geosci. Remote Sensing*, vol. 37, pp. 1204-1211, May 1999.